JOURNAL OF SOLID STATE CHEMISTRY 97, 292–298 (1992)

A Study of the Interaction of Li_2O and γ-Alumina

LIFENG ZHANG, JUNFAN LIN, AND YI CHEN[1]

Chemistry Department, Nanjing University, Nanjing 210008, China

Received September 26, 1991

Metal oxide–support interactions have been studied in γ-alumina-supported Li_2O samples, prepared by calcining γ-alumina impregnated with $LiNO_3$. Highly dispersed lithium nitrate can be decomposed at temperatures far lower than that of its bulk phase, and the lithium oxide thus formed interacts strongly with γ-alumina, since α-$LiAlO_2$ can be easily formed at a calcination temperature as low as 733 K. A method based on acid–base titration has been designed to evaluate the dispersion capacity of lithium oxide on γ-alumina, which is 11.3 Li^+ cations/100 m^2 γ-alumina, in good agreement with the value predicted by an incorporation model. © 1992 Academic Press, Inc.

Introduction

Metal oxide–support interactions have attracted much attention because of the wide application of supported-metal oxide systems. It has been well documented that under appropriate conditions many metal oxides can be dispersed on the surface and/or diffuse into the bulk of γ-alumina. However, the details of the interaction between metal oxide and support remains unclear, and a diversity and even contradiction of results and interpretations can be found in the literature. Xie and Tang (*1*) were the first to claim that the monolayer dispersion of many metal oxides on γ-alumina can be realized simply by the calcination of mechanical mixtures at ~770 K. Measurement of the dispersion capacity of many metal oxides, i.e., the maximum amount of atomically dispersed metal oxide without the existence of a bulk phase, by different experimental methods such as XRD, ESCA, and ISS, led them to propose a close-packed monolayer model to explain the dispersion capacities of some metal oxides on γ-alumina. The dispersion process has been described by Knözinger as the wetting of the surface of γ-alumina by metal oxides (*2*). It has also been commonly accepted that interactions between γ-alumina and the dispersed species are inevitable. In fact, it has been shown that the coordination environment of the metal cations dispersed on γ-alumina is strongly dependent upon their loading amount as well as the calcination conditions used (*3, 4*); therefore, the strong impact of these factors on the properties (e.g., reducibility, magnetic properties, catalytic activity, etc.) of γ-alumina-supported metal oxide systems can be expected.

Interactions between metal oxides and γ-alumina have been discussed in many papers (*5–7*) by taking into consideration the possibility of metal cations incorporating into the surface layer or even into the bulk phase of γ-alumina. We have recently reported (*8, 9*) that under appropriate experimental conditions, the interaction between

[1] To whom correspondence should be addressed.

0022-4596/92 $3.00

Copyright © 1992 by Academic Press, Inc.
All rights of reproduction in any form reserved.

many metal oxides and γ-alumina can be described by an incorporation model assuming that the (110) plane is preferentially exposed on the surface of γ-alumina; most of the experimental results which support this model are the dispersion capacities of oxides containing M^{2+} or M^{6+} cations and the relationship between the coordination environment and the loading amount of these metal oxides supported on γ-alumina.

Alkali promoters are often used for the purpose of improving the catalytic selectivity or activity of supported catalysts of industrial importance. The nature of the interaction between alkali promoter and support, which correlates directly to the location of the alkali cations in the catalyst, and the effect of the alkali promoter on the dispersibility and reducibility of the active components is important in gaining a deeper insight into the roles of these promoters in modifying catalytic behavior (*10*). In this paper Li_2O has been used to determine if the incorporation model can be used to describe the dispersion of M^{1+}-type oxides as well. Due to the fact that at normal calcination temperatures Li^+ cations not only can incorporate into the surface layer of γ-alumina but also diffuse into its bulk phase to produce α-$LiAlO_2$, a method based on acid–base titration has been developed to evaluate the dispersion capacity of Li_2O on γ-alumina.

Experimental

Samples were prepared by impregnating γ-alumina with aqueous solutions containing the appropriate amount of lithium nitrate; the solutions were then evaporated to dryness, and the samples were dried at 390 K and kept in a desiccator. The γ-alumina support (CP grade, E. Merck, Darmstadt) was precalcined at 973 K for 3 hr before impregnation, and the specific surface area of γ-alumina after calcination was 92 m^2/g.

A Shimadzu XD-3A X-ray diffractometer with Cu$K\alpha$ radiation (0.15418 nm) was used to obtain X-ray diffraction patterns. Differential thermal analysis was carried out in flowing N_2 with a scanning rate of 10 K/min using a CYR-1 (Shanghai) type thermoanalyzer.

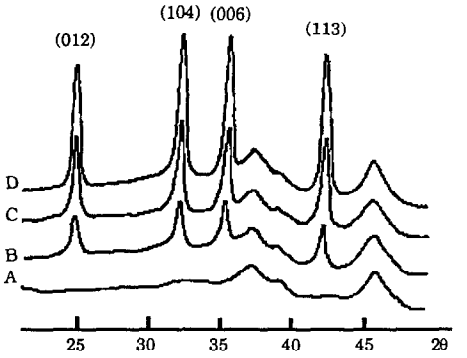

FIG. 1. XRD patterns of samples with $LiNO_3$ content of 1.0 (A), 2.0 (B), 4.0 (C), and 6.0 (D) mmol/g γ-alumina.

Results and Discussion

Figure 1 shows the X-ray diffraction patterns of γ-alumina impregnated with $LiNO_3$ before calcination. Apparently, the intensity of the peaks corresponding to bulk phase $LiNO_3$ increases with increased loading amount of $LiNO_3$, while at rather low loading, (<1.0 mmol/g γ-alumina), none of these peaks can be visualized. It is likely that $LiNO_3$ is highly dispersed on the surface of γ-alumina, either with the formation of a monolayer as suggested by Xie and Tang (*1*) or with the incorporation of Li^+ cations into the surface lattice of γ-alumina as suggested by Chen *et al.* (*8, 9*). As the loading amount of $LiNO_3$ is increased above its dispersion capacity, bulk phase $LiNO_3$ appears in addition to the highly dispersed species. It seems reasonable to suggest that the supported $LiNO_3$ can be considered as consisting in two forms: species that are in intimate contact with the surface of γ-alu-

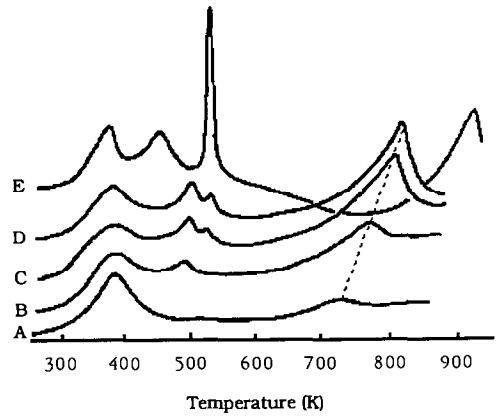

FIG. 2. DTA curves of $LiNO_3 \cdot H_2O$ (E) and $LiNO_3$/γ-alumina samples with $LiNO_3$ content of 1.0 (A), 2.0 (B), 4.0 (C), and 6.0 (D) mmol/g γ-alumina.

mina and other species that are actually located on the top of the first species and are less influenced by the support.

The DTA results of the above samples are shown in Fig. 2 together with the result of $LiNO_3 \cdot H_2O$ for comparison. For the case of unsupported $LiNO_3 \cdot H_2O$ the four endothermic peaks can be attributed respectively to the desorption of adsorbed water at ~373 K, the loss of crystallized water from the transformation of monohydrate to anhydrous lithium nitrate taking place at ~435 K, and the melting and decomposition of anhydrous lithium nitrate at ~528 and ~923 K. It is interesting to note that the DTA results of γ-alumina-supported $LiNO_3$ samples are strongly dependent on the loadings. For instance, only those peaks corresponding to the desorption of water and the decomposition of lithium nitrate were detected for low loading samples, as shown in Fig. 2 curve A; however, another two peaks (at ~493 and ~528 K) appear with the increase of loading amount, as seen in Fig. 2, curves C and D. Taking into account the fact that $LiNO_3$ is easily deliquescent in moist atmosphere, both of these two peaks are assigned to the melting of $LiNO_3$, noting that the peak at ~493 K is related to the amount of surface water and could shift to 528 K if the samples were further dried. The distinctive feature of the above results is that the decomposition temperatures of $LiNO_3$ in all the supported samples studied are lower than that of the bulk phase $LiNO_3$, i.e., the interaction between $LiNO_3$ and γ-alumina enhances the decomposition of $LiNO_3$.

The γ-alumina sample containing 6.0 mmol $LiNO_3$/g has been chosen as a representative to study the interaction between Li_2O and γ-alumina in samples prepared by the decomposition of supported $LiNO_3$. A comparison of the XRD patterns obtained after the samples had been calcined at 703 K for different periods is illustrated in Fig. 3. The intensities of the characteristic peaks of crystalline $LiNO_3$ decrease significantly during the first 30 min of calcination, and they are unchanged for longer times; moreover, no new crystalline phases were detected. Clearly, the results reveal that at 703 K the decomposition process stops after a definite amount of supported $LiNO_3$ has been decomposed. This result can be understood if the Li_2O produced remains on the surface and is sufficient to block the direct contact between γ-alumina and $LiNO_3$, thereby hindering the decomposition of the latter. Thus, one might expect that if the

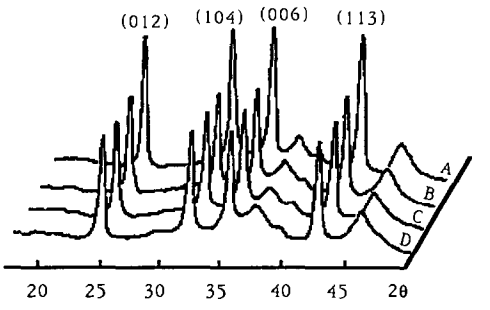

FIG. 3. XRD patterns of 6.0 mmol $LiNO_3$/g γ-alumina sample as prepared (A), and calcined at 703 K for 30 min (B), 60 min (C), and 90 min (D).

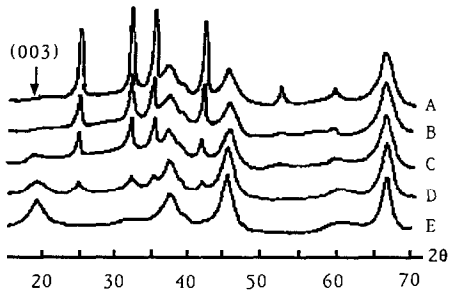

FIG. 4. XRD patterns of 6.0 mmol $LiNO_3$/g γ-alumina sample calcined at 783 K for 20 min (A), 40 min (B), 60 min (C), 90 min (D), and 150 min (E).

sandwiched Li_2O, or more possibly the Li^+ cations incorporated into the surface lattice of γ-alumina, can be removed, then the decomposition process should continue.

To investigate the effect of calcination temperature, the same sample was calcinated at 783 K, and the XRD patterns subsequently collected are shown in Fig. 4. In contrast to Fig. 3, the diffraction intensities of the characteristic peaks decrease continuously with the increase of calcination time, while new diffraction peaks with 2θ values at 37.7° (which overlaps with one of the characteristic peaks of $LiNO_3$), 45.3°, and 66.9° increase correspondingly. Moreover, after the sample was calcined at 783 K for 150 min, no residual crystalline phase of $LiNO_3$ could be detected, and the peak with $2\theta = 18.8°$ appears, corresponding to the diffraction of the (003) plane of α-$LiAlO_2$ appears. These facts suggest that at 783 K the diffusion of Li^+ cations into the bulk phase of γ-alumina leads to the formation of α-$LiAlO_2$ as well as renewing the intimate contact between the residual $LiNO_3$ and γ-alumina, which allows the further decomposition to continue. These results are consistent with Pott and Stork (*11*), who reported the formation of α-$LiAlO_2$ by the calcination at a temperature ~773 K of lithium carbonate supported on γ-alumina supported.

In view of the discussion presented above, a schematic description of the processes discussed can be drawn as shown in Fig. 5. In short, depending on the calcination temperature and time, two processes might occur on samples of γ-alumina impregnated with $LiNO_3$, i.e., the decomposition of the supported $LiNO_3$ and the diffusion of the surface Li^+ cations into the bulk of γ-alumina; the latter process leads to the continuous decomposition of $LiNO_3$ and the formation of α-$LiAlO_2$.

We have recently reported (*8*, *9*) that the dispersion capacities of metal oxides containing M^{2+} and M^{6+} cations on γ-alumina, measured for samples calcined at a typical temperature of ~770 K, are in good agreement with the values predicted by the incorporation model. It is therefore interesting to see whether the dispersion capacity of Li_2O on γ-alumina can also be described by this model. As discussed above, the diffusion of the Li^+ cations into the bulk phase of γ-alumina apparently occurs due to larger diffusivity of Li^+ cations on γ-alumina, even at a temperature as low as 783 K. In general, increasing the calcination temperature and the calcination time will result in more surface Li^+ cations diffusing into the bulk phase, which will lead to further $LiNO_3$ decomposition and even the formation of α-$LiAlO_2$. Accordingly, if the calcination temperature is high enough for the diffusion of Li^+ cations to occur, then the Li_2O produced by the decomposition of $LiNO_3$ on γ-alumina should distribute both on the surface and in the bulk of γ-alumina, i.e.,

$$LiNO_{3(\text{decomposed})} = Li^+_{(\text{surface})} + Li^+_{(\text{bulk})}.$$

Recall that

$$LiNO_{3(\text{decomposed})} = LiNO_{3(\text{impregnated})} - LiNO_{3(\text{residual})}.$$

Since the amount of impregnated $LiNO_3$ is known, one needs the value of $LiNO_{3(\text{residual})}$ to estimate the value of $LiNO_{3(\text{decomposed})}$. A method has been designed for this purpose. In particular, an excess

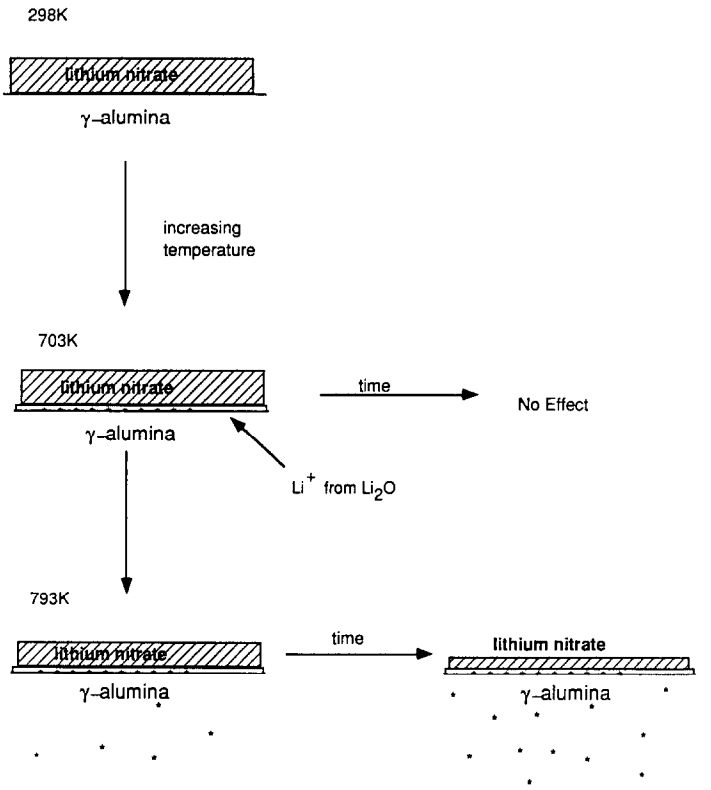

FIG. 5. Schematic representation of $LiNO_3$/g γ-alumina samples treated at different calcination conditions.

amount of distilled water was added to the calcined sample with constant mixing, and the resulting slurry was filtered. This procedure was repeated with distilled water for several times, and the solution thus collected was then neutralized by the titration with HCl solution. While the extraction process removes both residual $LiNO_3$ and at least part of the Li_2O from the sample, the HCl titration provides a measure of the latter amount, since Li^+OH^- (produced by the solution of Li_2O in water) is neutralized to Li^+Cl^- during the titration. The aqueous solution was subsequently evaporated to dryness, followed by calcination at 923 K. This treatment converted the residual $LiNO_3$ into Li_2O. The solid mixture was then dissolved in distilled water, and the Li_2O was titrated by the HCl solution, providing a measure of the original amount of residual $LiNO_3$.

The relationship of $LiNO_{3\text{decomposed}}$ with calcination time and temperature for the sample of γ-alumina containing 6.0 mmol $LiNO_3$/g is shown in Fig. 6. The results show that at temperatures ranging from 703 to 793 K, there is a linear relationship between the amount of $LiNO_3$ decomposed and the calcination time, and the higher the calcination temperature the larger the slope of the straight line. Most interestingly, all the above straight lines intersect at a point corresponding to a decomposition amount of 1.88 mmol $LiNO_3$/100 m^2 γ-alumina at zero calcination time. It is reasonable to think that diffusion into the bulk is not sig-

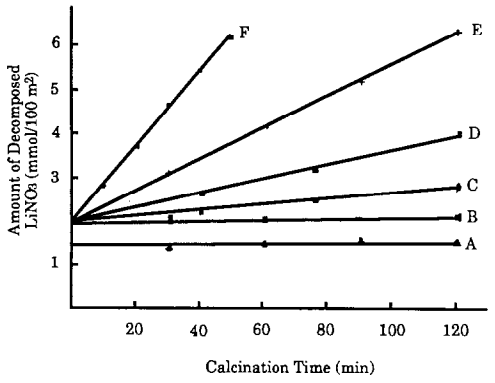

FIG. 6. The amount of decomposed $LiNO_3$ in 6.0 mmol $LiNO_3$/g γ-alumina samples vs calcination time for sample calcined at 683 K (A), 703 K (B), 733 K (C), 753 K (D), 773 K (E), and 793 K (F).

nificant at this point; therefore, the results suggest a dispersion capacity of 0.94 mmol Li_2O/100 m^2 γ-alumina or 11.3 Li^+ cations/100 m^2 γ-alumina. The different slopes of the straight lines in Fig. 6 apparently relate to the different diffusion rates of lithium cations at different temperatures. The low decomposition value for the sample calcined at 683 K could be correlated to the incomplete decomposition of $LiNO_3$ at such a low temperature.

As discussed previously with respect to the incorporation model (*8, 9*), metal cations can incorporate into surface vacant sites on the (110) plane of γ-alumina, and the oxygen anions associated with the cations stay at the top of the occupied sites as capping oxygens to compensate the positive charges. Due to the shielding effect of the capping oxygen anions, some of the available vacant sites are not usable, which explains the different dispersion capacities of M^{2+}- and M^{6+}-type metal oxides. For the case of Li_2O, two lithium cations share only one oxygen anion, and the shielding effect is accordingly less pronounced. However, the two opposite tetrahedral vacant sites on the surface lattice can only be occupied by one lithium cation because of steric hindrance (the radius of lithium cation is about 0.068 nm) as well as electric repulsion, which makes the dispersion capacity of Li_2O equal to 11.4–12 cations/nm^2, as shown schematically in Fig. 7. The above estimation is in good agreement with the experimental results.

Conclusions

1. $LiNO_3$ on γ-alumina decomposes at temperatures significantly lower than that of bulk phase $LiNO_3$, due to the interaction between lithium nitrate and γ-alumina.

2. The Li_2O produced by the decomposition of $LiNO_3$ supported on γ-alumina can

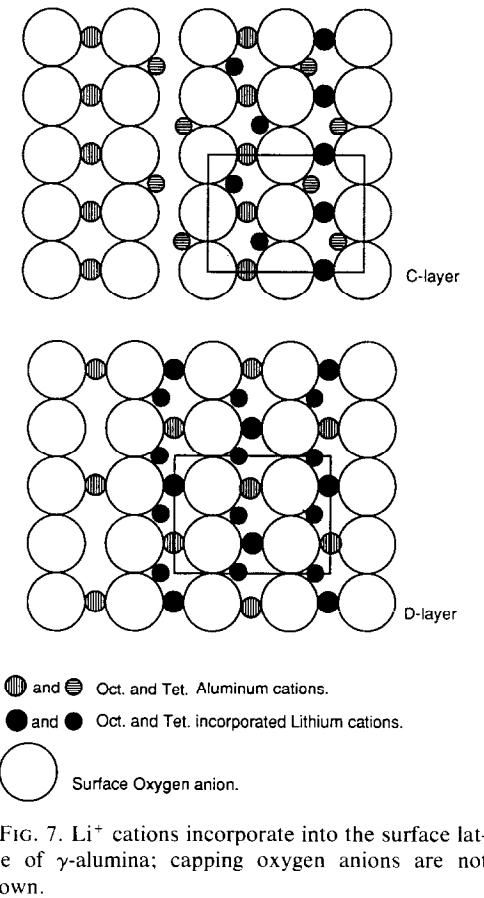

FIG. 7. Li^+ cations incorporate into the surface lattice of γ-alumina; capping oxygen anions are not shown.

incorporate into the surface lattice of γ-alumina and diffuse into the bulk with the formation of α-$LiAlO_2$ at fairly low temperatures (733–793 K).

3. The dispersion capacity of Li_2O on γ-alumina evaluated by the incorporation model is 11.4–12 cations/nm^2, in good agreement with the experimental results.

Acknowledgments

This work was supported, in part, by the National Natural Science Foundation of China. The authors acknowledge valuable discussions with Professor J. A. Dumesic and Mr. D. Chen during the visit of YC to the University of Wisconsin in the summer of 1991.

References

1. Y. C. Xie and Y. Q. Tang, *Adv. Catal.* **37,** 1 (1990).
2. H. Knözinger, *in* "Proceedings, 9th International Congress on Catalysis, Calgary, 1988" (M. J. Phillips and M. Teman, Eds.), Vol. 5, p. 20, Chem. Institute of Canada, Ottawa (1988).
3. D. S. Zingg, L. E. Makovsky, R. E. Tischer, F. R. Brown, and D. M. Hercules, *J. Phys. Chem.* **84,** 2898 (1980).
4. L. W. Burggraf, D. E. Leyden, R. L. Chin, and D. M. Hercules, *J. Catal.* **78,** 360 (1982).
5. M. Lo Jacono, M. Schivavello, and A. Cimino, *J. Phys. Chem.* **75,** 1044 (1971).
6. M. Wu and D. M. Hercules, *J. Phys. Chem.* **83,** 2003 (1979).
7. B. Delmon and M. Houalla, *in* "Preparation of Catalysts II" (B. Delmon, P. Grange, P. A. Jacobs, and G. Poncelet, Eds.), p. 447, Elsevier, Amsterdam (1979).
8. Y. Chen, L. F. Zhang, J. F. Lin, and Y. S. Jin, *in* "Catalytic Science and Technology" (S. Yoshida, N. Takezawa, and T. Ono, Eds.), Vol. 1, p. 291, Kodansha, Tokyo (1991).
9. Y. Chen and L. F. Zhang, *Catal. Lett.*, in press.
10. T. E. Hoost and J. G. Goodwin, Jr., *J. Catal.* **130,** 283 (1991).
11. G. T. Pott and W. H. J. Stork, *in* "Preparation of Catalysts" (B. Delmon, P. A. Jacobs, and G. Poncelet, Eds.), p. 537, Elsevier, Amsterdam (1976).